Available online at www.sciencedirect.com
ScienceDirect
Scripta Materialia 56 (2007) 585–588
Scripta MATERIALIA
www.actamat-journals.com

# Shear fatigue strength of a prismatic diamond sandwich core

F. Côté, V.S. Deshpande* and N.A. Fleck

*Cambridge University Engineering Department, Trumpington Street, Cambridge CB2 1PZ, UK*

Received 29 November 2006; revised 18 December 2006; accepted 20 December 2006
Available online 23 January 2007

The shear fatigue performance of stainless steel diamond cores has been measured and *S–N* curves reported for two core relative densities. The fatigue mechanism for the low relative density core involves the successive bending fatigue of constituent struts near the ends of the specimen, while the high density core fails by fatigue failure of the joints between the core and the face-sheets. A significant knock-down in the fatigue shear strength of the core is observed compared to its monotonic strength.


*Keywords:* Diamond core; Fatigue; Shear strength; Sandwich panels

Metallic micro-architectured materials are under development for multi-functional applications due to their ability to support loads, dissipate heat and undergo a shape change [1]. The three basic architectures are the truss [2], honeycomb [3] and prismatic core [4]. Their deformation response under quasi-static and dynamic loading has been the subject of numerous recent studies (see e.g. [5,6]).

Sandwich structures with lattice cores are commonly subjected to cyclic loading and consequently, their fatigue performance is of concern. The core is subjected to shear loading and hence the shear fatigue performance of the sandwich cores is of primary interest. Most of our current understanding of the fatigue of cellular metallic materials is guided by the existing literature on the fatigue properties of metallic foams. The tension–tension fatigue of metal foams is by cyclic ratcheting of the cell walls [7] while compression–compression fatigue failure occurs by the progressive development of crush bands [8]. In contrast, shear fatigue of metal foams involves the development of distributed tensile microcracks [9]. The endurance limit $\tau_e$ of Alporas aluminium alloy foam is $0.35\tau_p$, where $\tau_p$ is the peak monotonic shear strength. A recent study [10] on pyramidal lattice cores manufactured by cutting, folding and then brazing together AL6XN stainless steel sheets suggests that while the shear fatigue performance of these cores is governed by the fatigue strength of the brazed joint; the measured endurance limit $\tau_e/\tau_p \approx 0.3$ is similar to that of Alporas metal foam. Prismatic diamond cores are considered optimal for application as sandwich cores [11] due to their combination of high compressive, longitudinal shear and axial strengths. This study focuses on investigating the shear fatigue performance of sandwich cores with a diamond-like topology.

Prismatic diamond sandwich cores (Fig. 1) were manufactured from AISI type 304 stainless steel sheets of thickness $t = 0.3$ mm using the slotting technique (Fig. 1(a)) of Côté et al. [3]. Stainless steel sheets were cropped into rectangles, and then cross-slotted by electro-discharge machining (EDM). The slots were of width $\Delta t = 0.305$ mm and of spacing $l$, and were cut to half the depth of the sheet. The sheets were assembled in a $\pm 45°$ array in order to produce sandwich panels of length $L$, thickness $H$ and width $W$ (Fig. 1(a)). A clearance of 5 μm between the sheets and slots facilitated assembly whilst providing a sufficiently tight fit to assure stability. The braze alloy Ni–Cr 25–P10 (wt.%) was applied uniformly over the sheets of the core (increasing the sheet thickness to $t = 0.32$ mm) and over the inner surface of the steel face-sheets, of thickness $h = 3$ mm. The assembly (core and face-sheets) was brazed together in a vacuum furnace at 1075 °C in a dry argon atmosphere at 0.03–0.1 mbar. Capillarity forces were sufficient to draw the braze into the joints, resulting in an excellent bond. The quality of the braze joints was assessed by optical microscopy and scanning electron microscopy (SEM)/energy-dispersive X-ray (EDX) dot mapping techniques. The surface of a typical brazed cross-joint was prepared by successive grinding steps

* Corresponding author. Fax: +44 1223 332662; e-mail: vsd@eng.cam.ac.uk

1359-6462/$ - see front matter 
doi:10.1016/j.scriptamat.2006.12.035

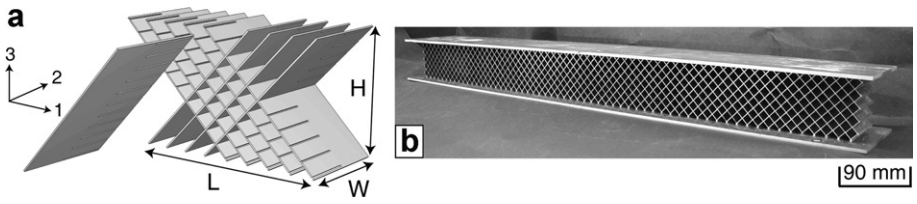


**Figure 1.** (a) Sketch of the slotting procedure used to manufacture the diamond core and (b) a photograph of an as-manufactured $\bar{\rho} = 0.08$ prismatic diamond core sandwich specimen.

and a final polish with 1 μm diamond paste. The polished surface was then etched using a solution comprising 74% chloridric acid and 1.3% hydrogen peroxide. An optical photograph of a polished and etched brazed joint shown in Figure 2 confirms the good overall bonding at the joints. Closer inspection, however, reveals the presence of two phases in the joint. The composition of those phases was obtained by EDX dot mapping analysis. One of the phases has approximately the same composition as that of stainless steel, i.e. Fe, Ni and Cr, while the second phase contains phosphides which are expected to decrease the ductility of the joint [12].

The relative density of diamond sandwich core specimens is given, to first order, by

$$\bar{\rho} = \frac{2t}{l \sin 2\omega} \tag{1}$$

where $\omega$ is the half angle between the cross-slotted sheets; all specimens considered here have cells with $\omega = \pi/4$.

The transverse shear ($\tau_{31}$ vs. $\gamma_{31}$) monotonic and fatigue performances of the prismatic diamond cores of relative density $\bar{\rho} = 0.08$ and $\bar{\rho} = 0.15$ were measured via single-lap shear tests (Fig. 3) conforming to the ASTM standard C273-94 [13] for shear tests on sandwich cores. The shear assembly comprised 25 mm thick steel platens that were arc-welded onto the face-sheets of the diamond core sandwich panel and the assembly was loaded under compression via cylindrical rollers (Fig. 3). The dimensions of the shear fixture were chosen such that, in accordance with the ASTM standard C273-94 [13], the load line coincided with a diagonal of the sandwich core specimen. Moreover, in order to minimize edge effects, the tests were performed on specimens with aspect ratio $L/H = 12$, 5 cells in the $x_3$-direction and width $W = 50$ mm. Both relative densities of sandwich cores were manufactured from $t = 0.3$ mm sheets and so the cell sizes were $l = 7.5$ and 4 mm for the $\bar{\rho} = 0.08$ and 0.15 diamond cores, respectively. The specimens of relative density $\bar{\rho} = 0.08$ and 0.15 were of lengths $L \approx 640$ and 340 mm, respectively.

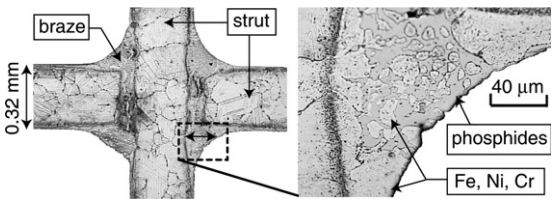


**Figure 2.** Optical photograph of a polished braze joint showing the effect of diffusion bonding on the microstructure of the joint. The magnified region reveals the presence of two phases in the joint.

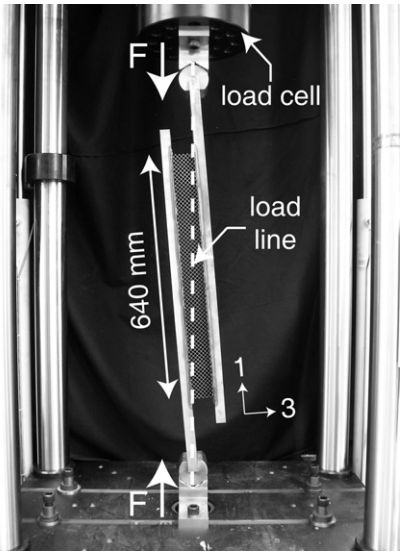


**Figure 3.** Photograph of a $\bar{\rho} = 0.08$ prismatic diamond core specimen in the single-lap shear test configuration. The load line and the direction of the applied load $F$ are marked.

The transverse shear monotonic and fatigue responses were measured using a servo-hydraulic frame test machine. The macroscopic shear stress on the core was inferred from the load cell of the test machine while the average through-thickness shear strain was measured by a clip gauge attached to the 25 mm thick plates of the shear test apparatus and straddling the core.

The monotonic transverse shear response (applied strain rate $\dot{\gamma}_{31} = 10^{-4}\ \mathrm{s}^{-1}$) of both the $\bar{\rho} = 0.08$ and 0.15 diamonds (Fig. 4) display a peak stress $\tau_p$ followed by softening. Images of the deformation at selected shear strain levels indicate that the peak stress is governed by the buckling of the constituent struts while

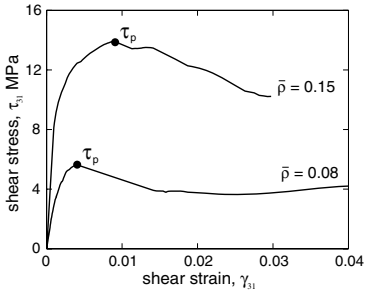


**Figure 4.** Measured monotonic shear responses of the $\bar{\rho} = 0.08$ and $\bar{\rho} = 0.15$ prismatic diamond cores. The peak shear stress $\tau_p$ is indicated on the curves.

the softening is associated with the post-buckling response and subsequent fracture of the brazed joints. The analytical and finite element calculations by Côté et al. [4] have shown that the $\bar{\rho} = 0.08$ core is at the transition between elastic and plastic buckling. By contrast, the $\bar{\rho} = 0.15$ diamond core collapses by plastic buckling.

Cyclic shear tests were conducted on the core using the same single-lap shear configuration as that used in the monotonic shear tests. The tests were conducted in the servo-hydraulic test machine in load control at 20 Hz. Define the load ratio $R$ as the ratio of minimum absolute applied shear stress $\tau_{\min}$ to maximum absolute shear stress $\tau_{\max}$, and define the shear stress range as $\Delta\tau \equiv \tau_{\max} - \tau_{\min}$. Fatigue tests were performed at $R = 0.5$ for the $\bar{\rho} = 0.08$ diamond core while the fatigue performance of the $\bar{\rho} = 0.15$ core was investigated for the two load ratios $R = 0.1$ and 0.5.

The shear strain at maximum load $\gamma_{\max}$ vs. the number of cycles $N$, at selected stress ranges $\Delta\tau/\tau_p$, is shown in Figure 5(a) for the $\bar{\rho} = 0.08$ core and a load ratio $R = 0.5$. The shear strain remains almost constant during an initial incubation period followed by a short period during which $\gamma_{\max}$ increases substantially with increasing $N$. Subsequently, there is a knee in the $\gamma_{\max}$ vs. $N$ curve and complete failure of the specimen follows shortly. Fatigue failure is defined by the number of cycles $N_f$ required for $\gamma_{\max}$ to attain the arbitrary but large value of 0.1. The fatigue life is relatively insensitive to the precise level of $\gamma_{\max}$ beyond the knee of the curve, due to the steeply rising character of the curve. The origins of fatigue failure of the $\bar{\rho} = 0.08$ core are traced back to the bending deformations induced in the constituent struts near the ends of the specimen [14]. During the initial incubation period, all struts of the core remain intact. Struts in the specimen interior undergo cyclic compression–compression or tension–tension loading, while struts near the ends of the specimen are subjected to cyclic bending and are the first to fail. The successive failure of struts starting at the free edge and propagating into the interior of the specimen (Fig. 6(a)) results in an increase of the effective compliance of the core: the shear strain $\gamma_{\max}$ increases with increasing $N$. Final fatigue failure of the specimen occurs by tearing of struts over the entire length of the specimen.

A representative SEM image of the fatigue fracture surface of a strut wall in the $\bar{\rho} = 0.08$ core is given in Figure 6(b) and clearly shows the crack trajectory. The fatigue crack propagated across the section of the strut and the residual ligament fails by ductile failure.

Next, consider the fatigue response of the $\bar{\rho} = 0.15$ diamond core. The $\gamma_{\max}$ vs. number of cycles, $N$, curves at selected values of $\Delta\tau$ are plotted in Figure 5(b) and (c) for $R = 0.1$ and 0.5, respectively. Again, the shear strain at maximum load, $\gamma_{\max}$, remains almost constant during an initial incubation period followed by a sudden sharp increase of $\gamma_{\max}$ due to fatigue failure in the brazed joints along the interface between core and face-sheets. Fatigue failure in the $\bar{\rho} = 0.15$ core is catastrophic and the intermediate regime where $\gamma_{\max}$ increases steadily with increasing $N$ is absent; compare Figure 5(a) with (b) and (c). The shear fatigue response and failure mechanism of the $\bar{\rho} = 0.15$ diamond core is similar to that of the $\bar{\rho} = 0.07$ pyramidal sandwich core [10]: for both $R = 0.1$ and $R = 0.5$, shear fatigue is by interfacial failure at the joints between core and face-sheets. The stocky nature of the constituent struts in the $\bar{\rho} = 0.15$ diamond core and the $\bar{\rho} = 0.07$ pyramidal core means that the brazed joints are heavily loaded and undergo

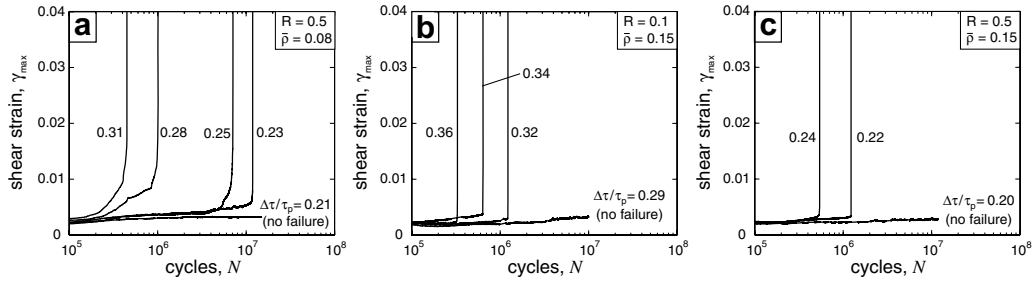


**Figure 5.** The accumulated maximum shear strain vs. number of cycles for selected shear stress ranges. (a) $\bar{\rho} = 0.08$, $R = 0.5$; (b) $\bar{\rho} = 0.15$, $R = 0.1$ and (c) $\bar{\rho} = 0.15$, $R = 0.5$.

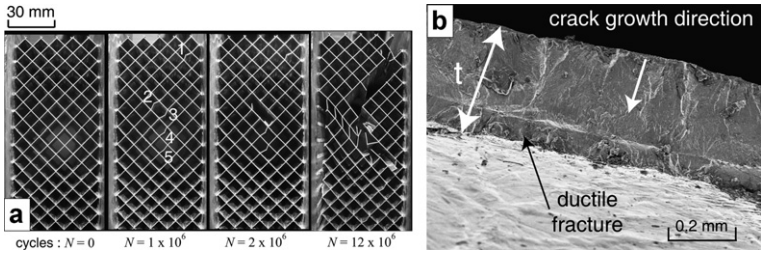


**Figure 6.** (a) Photographs of the end portion of the $\bar{\rho} = 0.08$ prismatic diamond core specimen tested at $\Delta\tau/\tau_p = 0.23$ and $R = 0.5$. The photographs show the sequence of fatigue failure from one strut to the next, within the sandwich core. The struts failed in the sequence 1–5 for cycling between $N = 1 \times 10^4$ and $N = 1 \times 10^6$. (b) SEM images of fatigue fracture surface of the strut that failed after $N = 1 \times 10^6$ cycles at the site marked 2 in (a).

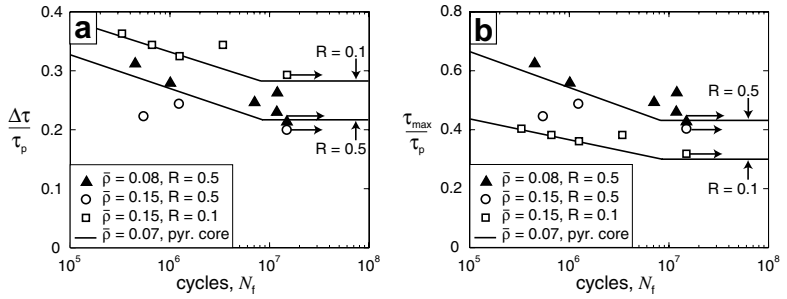


**Figure 7.** Transverse shear $S$–$N$ curves of the $\bar{\rho} = 0.08$ and 0.15 prismatic diamond core specimens plotted in terms of (a) the stress range $\Delta\tau$ and (b) the maximum stress $\tau_{max} \equiv \Delta\tau/(1 - R)$. Data for the $\bar{\rho} = 0.07$ pyramidal core [10] are also included as solid lines.

**Table 1.** Shear endurance ratios $\Delta\tau_e/\tau_p$ for a range of metallic sandwich cores

| Core topology | Parent material | $\bar{\rho}$ | $\Delta\tau_e/\tau_p$ ($R = 0.1$) | $\Delta\tau_e/\tau_p$ ($R = 0.5$) |
|---|---|---|---|---|
| Hexagonal honeycomb [15] | Aluminium | 0.04 | 0.31 | – |
| Alporas foam [9] | Aluminium | 0.11 | 0.31 | – |
| Pyramidal lattice [10] | AL6XN stainless steel | 0.07 | 0.27 | 0.20 |
| Diamond lattice | 304 Stainless steel | 0.08 | – | 0.21 |
| Diamond lattice | 304 Stainless steel | 0.15 | 0.29 | 0.20 |

fatigue failure. The presence of phosphides in the braze decreases the ductility of the joints [12] and degrades their fatigue strength [10].

The measured $S$–$N$ curves of the $\bar{\rho} = 0.08$ ($R = 0.5$) and $\bar{\rho} = 0.15$ ($R = 0.1$ and 0.5) prismatic diamond cores are plotted in Figure 7 in terms of both the stress range $\Delta\tau$ (Fig. 7(a)) and the maximum stress $\tau_{max} \equiv \Delta\tau/(1 - R)$ (Fig. 7(b)). The data are normalised by the monotonic peak shear strength of the respective cores (Fig. 4). The shear endurance limit $\Delta\tau_e$, as defined by the stress range at a fatigue life of $10^7$, is marked in Figure 7. In all cases, the shear endurance limit $\Delta\tau_e$ is below the monotonic shear yield strength. Although the fatigue mechanisms of the $\bar{\rho} = 0.08$ and 0.15 diamond cores at $R = 0.5$ are rather different, the $S$–$N$ curves for these materials overlap. The shear $S$–$N$ data for the $\bar{\rho} = 0.07$ pyramidal core [10] are included as solid lines in Figure 7; lines are given for $R = 0.1$ and 0.5, with $\Delta\tau$ normalised by the measured monotonic peak strength of the pyramidal core. The data of Figure 7 reveal that the normalised $S$–$N$ curve is sensitive to the load ratio $R$ (when either $\Delta\tau$ or $\tau_{max}$ is employed to define the endurance limit), but relatively insensitive to the core density and topology.

The shear fatigue performance of stainless diamond cores is compared with that for alternative cores in Table 1, which includes shear endurance data $\Delta\tau_e$ (for $R = 0.1$ and 0.5, as available) for AL6XN stainless steel pyramidal cores [10], aluminium hexagonal honeycombs [15] and Alporas aluminium metal foams [9]. The data for $\Delta\tau_e$ is normalised by the measured monotonic peak shear strengths $\tau_p$ of the respective cores. As already noted for the data of Figure 7, the tabulated data suggest that the normalised shear endurance limit $\Delta\tau_e/\tau_p$ is independent of the core topology, material and relative density $\bar{\rho}$. A significant knock-down factor in shear fatigue strength is evident for all the cores considered, including stochastic metal foams and the periodic lattice materials.

The authors are grateful to ONR for their financial support through US-ONR IFO grant number N00014-03-1-0283. F.C. acknowledges support from the Cambridge Commonwealth Trust and the Fonds Québécois de la Recherche sur la Nature et les Technologies.

[1] A.G. Evans, J.W. Hutchinson, N.A. Fleck, M.F. Ashby, H.N.G. Wadley, Progr. Mater. Sci. 46 (2001) 309.
[2] V.S. Deshpande, N.A. Fleck, M.F. Ashby, J. Mech. Phys. Solids 49 (2001) 1747.
[3] F. Côté, V.S. Deshpande, N.A. Fleck, A.G. Evans, Mater. Sci. Eng. A 380 (2004) 272.
[4] F. Côté, V.S. Deshpande, N.A. Fleck, A.G. Evans, Int. J. Solids Struct. 43 (2006) 6220.
[5] V.S. Deshpande, N.A. Fleck, Int. J. Solids Struct. 38 (2001) 6275.
[6] D.D. Radford, N.A. Fleck, V.S. Deshpande, Int. J. Impact Eng. 32 (2006) 968.
[7] A.-M. Harte, N.A. Fleck, M.F. Ashby, Acta Mater. 47 (1999) 2511.
[8] Y. Sugimura, A. Rabiei, A.G. Evans, A.-M. Harte, N.A. Fleck, Mater. Sci. Eng. A 269 (1999) 38.
[9] A.-M. Harte, N.A. Fleck, M.F. Ashby, Int. J. Fatigue 23 (2001) 499.
[10] F. Côté, N.A. Fleck, V.S. Deshpande, Int. J. Fatigue, in press.
[11] L. Valdevit, J.W. Hutchinson, A.G. Evans, Int. J. Solids Struct. 41 (2004) 5105.
[12] W.D. Zhuang, T.W. Eagar, Weld. J. 76 (1997) 157.
[13] ASTM Standard C273-94, Standard Test Method for Shear Properties of Sandwich Core Materials, American Society for Testing and Materials, West Conshohocken, PA, 1994.
[14] M. Zupan, V.S. Deshpande, N.A. Fleck, Eur. J. Mech. A/Solids 23 (2004) 411.
[15] F. Werren, Shear-Fatigue properties of various sandwich constructions, Report 1837, US Forest Products Laboratory, Madison, WI, 1952.